ELSEVIER

Journal of Fluids and Structures 19 (2004) 63–72

JOURNAL OF FLUIDS AND STRUCTURES

www.elsevier.nl/locate/jnlabr/yjfls

Wavelet analysis of sound signal in fluid-filled viscoelastic pipes

M. Prek*

Faculty of Mechanical Engineering, University of Ljubljana, Askerceva 6, Ljubljana SI-1000, Slovenia

Received 30 September 2002; accepted 25 September 2003

Abstract

In viscoelastic pipes, where the material properties depend on a complex bulk modulus as well as on a complex shear modulus, the sound field within the fluid is affected. Therefore, the dispersion of flexural waves occurs in the pipe, while the speed of flexural waves decreases due to the coupled fluid mass. Coupling between the pipe wall and the fluid also decreases the sound speed in the fluid. Likewise, the speed of sound in fluid is frequency dependent, just as the group velocity of bending waves depends on the frequency. Wavelet transform of nonstationary sound signal was used to identify the frequency-dependent fluid sound speed. Measurement and analysis of nonstationary signals with the use of time–frequency method provides a view to frequency-dependent transfer characteristics of fluid–pipe coupled system. The so-called fluid mode and pipe mode resonant frequencies are evident and the impact of different pipe wall material properties is shown. The results also showed that, in the case of propagating small disturbances (such as acoustic waves), the pipe wall inertance has a minor influence on the wave propagation characteristics. The elastic reaction of the wall to expansion of the cross section greatly exceeds the inertial reactions.

1. Introduction

Vibro-acoustic energy travels not only as sound waves through a fluid medium, but also as longitudinal and flexural waves through the pipe walls. Longitudinal waves in the pipe wall are coupled to the sound waves inside according to Poisson's ratio. One of the most common examples of this form of interaction is observed in water-filled pipes in which the flexibility of the walls significantly alters the speed of propagation of acoustic disturbances along the pipe. This interaction is most evident in viscoelastic pipes, which takes into account the effect of the viscoelasticity of the pipe wall material on the wave propagation. Although it is well known that the nonlinearity of pipe wall materials and the dynamic effects of pipe walls may result in a frequency-dependent wave speed, there has not been much research in this field. Fanelli (1973) has shown theoretically that the dynamic effect of the rock mass surrounding a rock-bored penstock led to a complex-valued and frequency-dependent Young's modulus for the wave speed. Similarly, Fanelli et al. (1983) reported on an experimental method applied to a laboratory perspex pipeline. The wave speed in the pipeline was frequency-dependent and complex valued as a consequence of the hysteretic and dynamic properties of perspex. Franke and Seyler (1983) adopted a frequency-dependent damping factor to compute hydraulic transients in viscoelastic pipes. They used the impulse response method instead of the standard method of characteristics (MOC). In the MOC, a term representing the retarded wall deformation is included and evaluated using the creep compliance of the wall material by means of Kelvin-Voigt elements. Rieutord and Blanchard (1979) adapted the standard MOC and presented a theoretical study of the effect of the viscoelastic properties of the wall material on transients. Galley et al. (1979) compared the calculated water hammer in polyethylene pipes with laboratory test data. Güney (1983) proposed a modified MOC model which took into account the effects of time-varying diameter and thickness and

*Tel.: +386-61-1771-200; fax: 386-61-218-567.
E-mail address: matjaz.prek@fs.uni-lj.si (M. Prek).

0889-9746/$ - see front matter © 2003 Elsevier Ltd. All rights reserved.
doi:10.1016/j.jfluidstructs.2003.09.003

frequency-dependent friction. Ghilardi and Paoletti (1986) investigated the application of viscoelastic pipes added to pipeline systems as suppressers of pressure surges.

In methods based on frequency response, the effect of viscoelastic properties is modelled through a frequency-dependent wave speed and a separate frequency-dependent damping factor. Meissner (1976) derived the wave speed and damping factor for an oscillating pressure wave propagating in a thin-walled viscoelastic pipe by incorporating the complex creep compliance into the unsteady momentum and continuity equations. Hirschmann (1979) has studied the resonating conditions in viscoelastic pipes with a modified impedance method, using frequency-dependent wave speed and a damping factor. The impulse response method has been utilized by Franke and Seyler (1983) to calculate the water hammer. Similarly, an impulse response method applied to compute nonperiodic transients has been proposed by other authors, e.g., Suo and Wylie (1989, 1990). The complex wave speed (complex valued and frequency dependent) is used in the standard impedance or transfer matrix method to analyze the oscillatory flow. A similar method has been proposed by Munjal and Thawani (1997) who applied the concept of transmission loss instead of the concept of wall impedance. An extended method, which uses the static mechanical properties and frequency-dependent mechanical properties of the pipe wall, has been proposed by Yu and Kojima (1998).

In this work the pulse method was used to measure propagation characteristics. An experimental study of axisymmetric propagation modes in fluid-filled viscoelastic pipe with emphasis on the two modes that exist down to the zero frequency limit is described. Thus two different waves of circumferential order 0 can propagate simultaneously. In order to investigate this, one could observe propagating acoustic pulses separated by a significant distance. The two modes, which travel at different speeds, would separate and their relative amplitudes could be measured. In our case the wavelet analysis was applied to the acoustic signal in order to analyze the structural features of the fluid-filled viscoelastic pipes, since the wavelet transform permits the characterization of a one-dimensional acoustic signal as a two-dimensional representation, evolving with time and period (frequency).

2. The time–frequency analysis methods

The practical objective is to extract as much information as possible from the measured results. The data may be short in duration because the phenomenon it represents happens quickly, or the characteristics of the measured data may change with time because of the changes in its underlying physical cause. Since classical methods (such as Fourier transform) have difficulty to handle transient signal analysis, time–frequency or time–scale analysis is more suitable for preserving high-frequency contents of the information carried by transient signals. Comparing with Fourier transform, the time–frequency/time–scale transform of a transient signal may detect and locate changes of the signal better than Fourier transform. One of the important applications of time–frequency/time–scale transform is the detection and extraction of unknown signal in noise. The localization of the time and frequency by time–frequency/time–scale transform makes it possible for de-noising, signal detection and extraction in the time–frequency domain. Feature extraction in the time–frequency domain refers to the identification of specific feature attributes from the transform domain. To recover and isolate specific signal features, the transform pairs must be not only effective, but also computationally efficient. A simple Fourier analysis of nonstationary signals, based on a joint time–frequency signal representation, is the use of the short-time Fourier transform (STFT). For a given signal $x(t)$, the STFT(t,f) is defined as

$$\mathrm{STFT}(t,f) = \int_{\tau} x(t+\tau)g(\tau)\mathrm{e}^{-\mathrm{i}2\pi f t}\,\mathrm{d}\tau, \tag{1}$$

where $g(\tau)$ is some arbitrary gate function. If the gate function is Gaussian, then the STFT is called a Gabor transform. However, the problem with the STFT is the length of the desired segment. Choosing a short analysis window may cause poor frequency resolution. On the other hand, a long analysis window may improve the frequency resolution but compromises the assumption of stationarity within the window.

Windowing techniques based on the choice of weighting function (or window function) are used in creating spectrograms, which have the purpose of giving a good simultaneous resolution in time and frequency. This is done by plotting the spectra obtained by sliding a weighting time window along the signal of interest and applying a STFT (or windowed Fourier transform) to each windowed segment, finally giving a plot of slices of time-varying spectra. The major drawback of STFT is on its constant time and frequency resolutions, as is presented by Newland (1994). To overcome the limitation of conventional analyzing technique for nonstationary signals, the Wigner-Ville distribution, described in, for example, Martin and Flandrin (1985), Andria et al. (1994) and wavelet analysis have been introduced.

2.1. Wavelet transform

The wavelet transform (WT), as introduced by Morlet et al. (1982) and Grossmann and Morlet (1984), is a technique for analyzing multiscale signals. Wavelet analysis in engineering, especially in the field of fluid mechanics, have been presented by Farge (1992) and Farge et al. (1996). Wavelets are able to decompose arbitrary signals into localized contributions that can be labeled in terms of time and scale, thus overcoming the limitations of Fourier analysis.

Wavelet transform provides a two-dimensional unfolding of one-dimensional signals, resolving both the position (in time or space) and the scale as independent variables, as is described by Mallat (1999). This method creates an expansion of an arbitrary real-valued function $f(t)$ over wavelets, constructed from a single function $\psi(x, s)$ by means of dilatations and translations (x and s are the wavelet analyzing position and scale). The basic wavelet function is a normalized function (i.e., the norm is 1) with an average value of zero:

$$\int_{-\infty}^{+\infty} |\psi(t)| \mathrm{d}t = 1, \tag{2}$$

$$\int_{-\infty}^{+\infty} \psi(t)\, \mathrm{d}t = 0. \tag{3}$$

The wavelet transform W_f of the arbitrary function $f(t)$ with respect to the wavelet $\psi(x, s)$ is defined as

$$W_f(x, s) = \int f(t)\psi^*[(t - x)/s]\, \mathrm{d}t, \tag{4}$$

where the asterisk indicates the complex conjugate. The wavelet ψ is a regular function, localized around $x = 0$. The choice of the appropriate wavelet functions depends on the kind of information that we want to extract from the signal. Of these possible functions, the Mexican hat, and the Morlet and Gabor functions are often applied in the field of fluid mechanics.

The analysis was performed by using Morlet wavelet function $\psi(\tau)$, which depends on a nondimensional "time" parameter τ. The Morlet wavelet consists of a plane wave modulated by Gaussian, such that

$$\psi(\tau) = \pi^{-1/4} \mathrm{e}^{\mathrm{i}\omega_0\tau}\, \mathrm{e}^{-\tau^2/2}, \tag{5}$$

where ω_0 is nondimensional frequency—in our case $\omega_0 = 6$ to satisfy the admissibility condition defined by Eq. (3). To ensure that the wavelet transforms at each scale s are directly comparable to each other and to the transforms of other time series, the translated and dilated wavelet function is normalized to have unit energy. Since the norm of the Morlet wavelet function is π, we can normalize it by multiplying with $1/\sqrt[4]{\pi}$. The continuous wavelet transform based on the Morlet wavelet has the benefit of a computational closeness to the Fourier modes. Indeed, $\omega = 2\pi/s$ can be interpreted as a local angular frequency. The advantage of this method, compared to the (windowed) Fourier transform, is that the time resolution adapts itself to the frequency. The time and angular frequency resolutions are respectively $\Delta\tau = 2s$ and $\Delta\omega = \omega/4$. Morlet wavelets provide the best compromise between time and frequency resolution, i.e., they minimize the product $\Delta\omega\Delta\tau = \pi$, independent of s. The time resolution is variable with frequency, so that high frequencies have a sharper time resolution.

The continuous wavelet transform $W_n(x_n, s)$ of a discrete sequence x_n (where $x_n = f(n\delta t)$) is defined as the convolution of x_n by a scaled and translated version of wavelet function $\psi(\tau)$ as

$$W_n(x_n, s) = \sum_{n=0}^{N-1} x_n \psi^* \left[\frac{(n' - n)\delta t}{s}\right]. \tag{6}$$

By varying the wavelet scale s and translating along the localized time index n, one can construct a picture showing both the amplitude versus the scale and how this amplitude varies with time. The set of scales s for use in the nonorthogonal wavelet analysis were defined as fractional powers of two:

$$s_j = s_0 2^{j\delta j},\ j = 0, 1, \ldots,\ J,$$
$$J = \frac{1}{\delta j} \log_2 \left(\frac{N\delta t}{s_0}\right), \tag{7}$$

where s_0 is the smallest resolvable scale and J determines the largest scale. The s_0 was chosen so that the equivalent Fourier period (for the Morlet wavelet where $\omega_0 = 6$, it gives the Fourier period 1.03 s) is approximately $2\delta t$. Adequate sampling within the scale is provided by a δj of about 0.5 for the Morlet wavelet. Smaller values of δj give finer resolution; to provide a smooth picture of wavelet power, $\delta j = 0.25$ was used in the analysis.

3. Influence of viscoelastic pipe material on wave propagation

3.1. Wave propagation in fluid-filled pipe

From an acoustical point of view the liquid is a state intermediate between a gas and a solid. It is gaslike and in the absence of losses it does not offer resistance to shear stress. Thus, the speed of sound in a fluid can be derived from the linearized, inviscid momentum equation (in the case of one-dimensional unsteady flow) and the continuity equation:

$$\frac{\partial p}{\partial x}+\rho\frac{\partial v}{\partial t}=0, \tag{8}$$

$$\frac{\dot{\rho}}{\rho}+\frac{\dot{S}}{S}+\frac{\partial v}{\partial x}=0, \tag{9}$$

where ρ is fluid density, v and p are average displacement velocity and pressure, S is the cross-sectional area of the pipe, t is time, x is the distance along the pipe and a dot over a variable represents the material derivative—a time derivative of states associated with particles rather than position (Lagrangian description). For liquid flow, Eq. (9) is rewritten as

$$\dot{p}+\rho\left[\frac{B/\rho}{1+(B/S)(\dot{S}/\dot{p})}\right]\frac{\partial v}{\partial x}=0, \tag{10}$$

where B is the bulk modulus of the fluid. Assuming a cylindrical pipe and linear dependency between pressure and pipe cross-section area change, Eq. (10) yields the following form:

$$\frac{\partial p}{\partial t}+\rho c_e^2\frac{\partial v}{\partial x}=0, \tag{11}$$

where c_e is the corresponding (equivalent) wave speed, defined as the bracketed term in Eq. (10); eliminating p from Eqs. (8) and (11) yields to following form:

$$\frac{\partial^2 v}{\partial t^2}=c_e^2\frac{\partial^2 v}{\partial x^2}. \tag{12}$$

Due to transverse strain and curvature, there is a coupling between pipe wall bending and longitudinal waves in pipe wall. That means the motion of the pipe wall is both normal and tangential to its surface. The ratio of the two components of motion is frequency dependent. Therefore the dispersion of a bending wave in a fluid-loaded pipe will be affected by the complex dynamic modulus.

3.2. Influence of viscoelastic properties

Although the stress is not directly proportional to strain, it is convenient in dealing with very small deformation of material with both elastic and viscous nature to combine a linear, Hookean stress–strain relationship with linear, Newtonian viscous relationship in order to determine the behavior of real material. Maxwell's element is a simple one combining one viscous parameter and one elastic parameter. Mechanically it can be illustrated as the Hookean spring and a Newtonian dashpot in series.

If sinusoidal force acts on a Maxwell element, the resulting strain will be sinusoidal at the same frequency, but out of phase. The resulting stress will be proportional to the Young's modulus E; the magnitude will be affected by relaxation time and will lead the strain. A common notation for this behavior is the complex dynamic modulus E^* (Eq. (13)), which is made up of a dynamic (storage) modulus E' and a loss modulus E'' as follows:

$$E^*=E'+\mathrm{i}E'' \text{ or } E^*=E'(1+\mathrm{i}\eta). \tag{13}$$

The loss modulus E'' is a measure of energy lost per cycle per unit volume and η is the loss factor. The variations of E', E'' and loss angle δ with relaxation time θ and frequency ω are shown in Fig. 1.

The effect of the viscoelasticity of the pipe wall material could be turned into the effective sound speed in pipe wall c_w:

$$c_w=\sqrt{\frac{E^*}{\rho_p}}, \tag{14}$$

where the ρ_p is the density of the pipe wall. The pressure dependency of the pipe cross-section could be defined by the complex Young's modulus. In this case, the compliance of the pipe wall is built into a effective (modified) bulk modulus for the fluid B_{eff}. Since the speed of sound in a fluid is a function of the fluid density ρ and the effective bulk modulus,

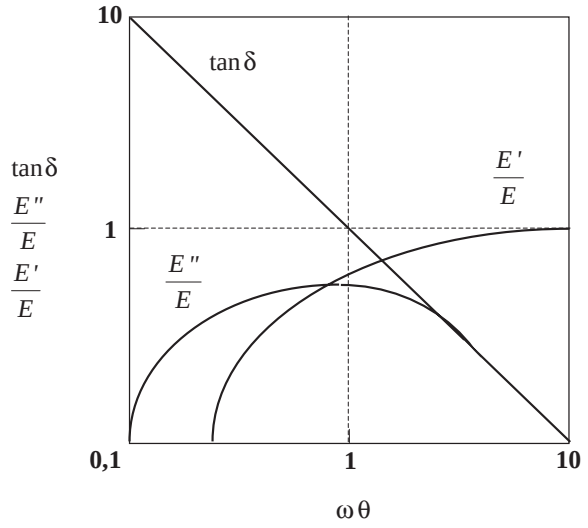

Fig. 1. The dependency between dynamic modulus E', loss modulus E'' and loss angle $\tan\delta$ as function of product $\omega\theta$.

we can define the corresponding (equivalent) wave speed as

$$c_e = \sqrt{\frac{B_{\text{eff}}}{\rho}}. \tag{15}$$

The structural damping is also accounted for by means of the modified (effective) bulk modulus. The effect of wall impedance appears only in the mass continuity equation. This inertial loading can greatly reduce modal natural frequencies, especially for low circumferential order. For thin-walled cylindrical structures, the inertial loading is roughly equal to an additional mass (pipe wall) per unit length. Well below the ring frequency of the pipe wall, the elastic reaction of the wall (to expansion of the cross section) greatly exceeds the inertial reaction. A simple model of this reaction, which only accounts for the elastic reaction of the pipe wall and neglects inertial effects, yields the following expression for wave speed (Korteweg-Lamb formula):

$$c_e \approx \frac{c}{\sqrt{1 + 2a\rho c^2/h\rho_p c_p^2}}, \tag{16}$$

where ρ_p and c_p are, respectively, the density and speed of sound (phase speed) in the pipe material, a and h are pipe mean radius and pipe wall thickness. A more comprehensive model, which also accounts for the influence of inertial reaction of the pipe wall on wave propagation, has been given by Munjal and Thawani (1996):

$$c_e = \frac{c}{\sqrt{1 - 2\mathrm{i}\dfrac{\rho c}{(\omega/c)r_i(\mathrm{i}\omega I + 1/\mathrm{i}\omega C)}}}, \tag{17}$$

where r_i is the internal pipe radius, I is the pipe mass per unit area of the wall (inertance) and C is the pipe compliance (radial deflection per unit pressure).

4. Experiment

4.1. Experimental procedure

In the investigation, the wavelet transforms were performed on the exponentially time-decaying frequency-dependent signals. The focus was on how these transforms reveal the time variations of the spectral content and the decay of the signals. To achieve the frequency-dependent signal, pipe with viscoelastic properties has been chosen. For comparison, three different pipe materials with different properties were examined. All pipes had a nominal diameter 1'' and were

designed for use in water supply installation. The copper (Cu) pipe with dimensions 32×1 mm represented the standard copper pipe material; the other two pipes are made of polypropylene (PP) with nominal diameter 32 mm and wall thickness 5.4 mm and polybutilene (PB) with nominal diameter 32 mm and wall thickness 3 mm. A 2.1 m long pipe of circular cross-section was filled with water and suspended vertically on foam pad. One end of the pipe was tapped lightly and the hammer (B&K type 8202) had a soft tip designed so that only low frequency disturbances were generated. The output from the hammer was also used for triggering. An hydrophone was mounted at the center of the pipe close to the point of impact. Measurement configuration consisted of a hydrophone (Brüel & Kjær type 8103) in conjunction with the charge amplifier (B&K type 2626), the FFT analyzer (B&K type 2032) and PC for additional computations.

For time varying signals a statistical approach must be taken with sufficient data accumulated to confidently make judgment regarding the measurement. The fast Fourier transform (FFT) analysis of transients is particularly straightforward when the entire transient fits into the transform size without loss of significant high-frequency information. For B&K type 2032 FFT analyzer the sampling frequency was 65 kHz, while the chosen frequency span 12.8 kHz included all relevant frequency information. The sampling interval was 30.5 μs and record length 62.5 ms. Transient analysis of measurement data were done with rectangular window as it provide equal weighting across the measurement period. The excited acoustic waves were registered and the input signal of 2048 samples has been processed.

4.2. Results and discussion

For analysis where a predetermined scaling may not be appropriate because of a wide range of dominant frequencies, a method of time–frequency localization that is scale independent, such as WT, should be employed. As mentioned, the Fourier transform is performed on a sliding element of length T from a time series of a time step δt and total length $N\delta t$, thus returning frequencies from $T-1$ to $(2\delta t)-1$ at each time step. At this analysis, according to Eq. (7), the scales varied from 20 Hz to 11.58 kHz. The frequency resolution of the Morlet wavelet (Eq. (5)) is approximately $\delta f = f/4$ and the time resolution is $\delta t = 2a$. Note that $\delta f \delta t = 1/2$, independent of a. The length of the Morlet wavelet used in the analysis affects the resulting time–frequency representation in the same way that the window length affected it in the STFT. This is because the wavelet is really acting as a window function, but is being used in a slightly different way. Where the FFT of the windowed portion of the signal is taken in the WT, the correlation between the signal and all the dilated versions of the wavelet at the same point in time is computed. This shows that an increase in wavelet length will give increased frequency resolution, but a decrease in time resolution, as is given by Newland (1999).

When the data are analyzed by described algorithm, the time–frequency map is generated. This is a contour map of a three-dimensional surface obtained by plotting the magnitude of the wavelet coefficients against time and frequency. The real part of wavelet coefficients are displayed, where the abscissa is time and ordinate is frequency (or period). For the WT map, the ordinate is logarithmic since the bandwidth in wavelet transform is constant over logarithmic scales. The time–frequency (or scale) representation of the energy concentration of the WT is called the ridge. The dominant features of each map are extracted by identifying correlation peaks. Each peak in the WT map represents the arrival time of a wave traveling with the group velocity. Ridges are described with the use of curves $s = s(x)$. In other words, ridges represent the frequency content of the analyzing signal with a high density of energy, which is dependent on time.

The absolute value of the WT is plotted in logarithmic scale as a function of the time-shift coefficient and the dilation coefficient. Contour plot of the WT represents the time–scale representation of the signal. Using the time–frequency distribution of the magnitude of the WT, analysis of dependency on frequency of group velocity and attenuation can be evaluated. For a harmonic waves propagating in L direction with small angular frequency difference $\Delta\omega$, the group velocity c_g at the mean angular frequency ω_g can be defined as $c_g = \Delta\omega/\Delta k$, where k is the wave number. The magnitude of WT takes its minimum value at $s = \omega_0/\omega_g$ and $x = (\Delta k/\Delta\omega)L = L/c_g$. Therefore, for a fixed distance L, a three dimensional plot of $|W_n(x_n, s)|$ on the (x, s) plane has a peak at $(x, s) = (L/c_g, \omega_0/\omega_g)$. In other words, the location of the peak on the WT map indicates the arrival time $x = Lc_g$ of the wave having angular frequency $\omega_g = \omega_0/s$.

Light gray and white regions of the graph presents the positive wavelet coefficients, dark gray and black regions the negative values. The analyzed signal is interesting because it disguises the passage of acoustic waves of different frequencies backwards and forwards along the pipe. When the impulse is applied first, acoustic waves travel along the pipe until they are reflected at the other end. Then they are returned to the point of impact, before being reflected again at the first end of pipe. Because the group velocity of flexural waves depends on frequency, high frequency waves travels faster than low frequency waves. Therefore a time–frequency map show more reflections for high frequency waves. Successive reflections of these appears as families of high wavelet coefficients at the same frequency.

In Fig. 2(b) is shown the wavelet transform of acoustic signal (Fig. 2(a)) in copper pipe. Only the frequency range of interest is shown, namely between 20 and 2900 Hz. As is evident from the map, the positions of ridges and courses

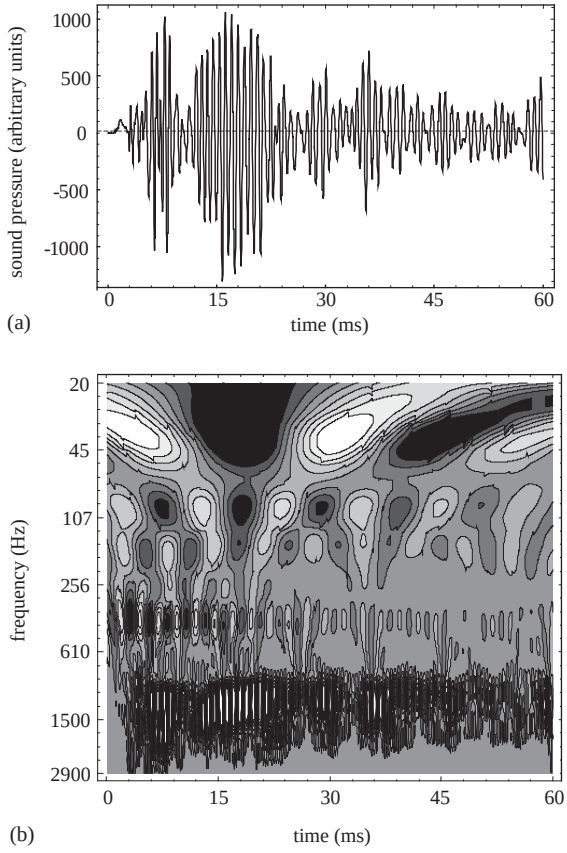

Fig. 2. Measured sound pressure signal and wavelet transform of signal in copper pipe: (a) pressure signal; (b) wavelet transform.

(negative ridges) are important. For ridges that run approximately parallel to the time axis, their position is identified by the maxims of sections cut parallel to the frequency axis. The correlation peaks follow the level and shows no change in scale. The time constant of the impulse and the location in time of the first and subsequent reflections of acoustic waves are clearly identified. By measuring the time separation between ridges at given frequency, the wave velocity at that frequency can be calculated. The distance in the time interval between two adjacent ridges is twice the length of the pipe. The estimated speed of traveling acoustic wave was $1240(+122/-86)$ m/s at 95% confidence interval, while no significant wave attenuation was observed in the measuring frequency range. The confidence interval is defined as the probability that the true wavelet power at a certain time and scale lies within a certain interval about the estimated wavelet power. The confidence interval for the "true" wavelet power, defined as $Wt_n^2(x_n, s)$, is then

$$\frac{2}{\chi_2^2(P/2)}|W_n(x_n,s)|^2 \leqslant Wt_n^2(x_n,s) \leqslant \frac{2}{\chi_2^2(1-(p/2))}|W_n(x_n,s)|^2, \tag{18}$$

where p is the desired significance ($p = 0.05$ for the 95% confidence interval) and $\chi_2^2(P/2)$ represents the value of χ^2 at $p/2$.

The second set of experiments was made with polybutilene (PB) and polypropylene (PP) pipe, while all other measuring parameters were the same as for the copper pipe. In propagating through solid materials, acoustic waves may have velocities that are dependent on their frequency. This dispersion may be due to the material behavior, such as in viscoelastic materials. There are two significant phenomenon that appear when the pipe wall yield. With rigid walls, the lowest order mode is truly a plane wave mode, but with elastic walls, the lowest order mode exhibits a dispersive sound speed, which is at all frequencies slower than the free field value. With rigid walls, the higher order modes exhibit a cut-off frequency, that is, there is a frequency below each higher order mode will not propagate, hence at low frequencies, the plane wave mode exists alone. With elastic walls, this is no longer true. At least one higher order mode can exist down to zero frequency. To clarify the impact of the viscous effect of the pipe material, the operating conditions were

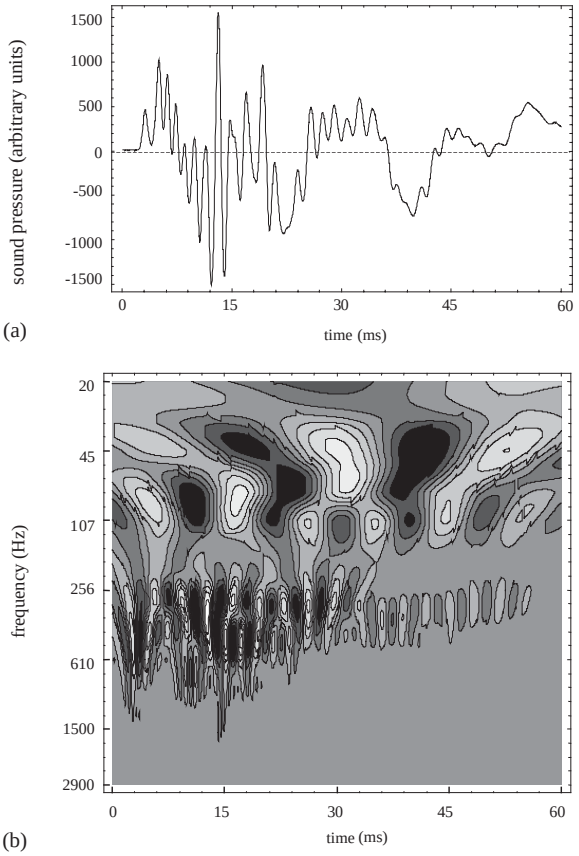

Fig. 3. Measured sound pressure signal and wavelet transform of signal in polybutilene (PB) pipe: (a) pressure signal; (b) wavelet transform.

made the same for all measurements. The main difference was in pipe material and this difference must reflects also in wavelet transform map. The wavelet transform of sound signal for PB pipe is shown in Fig. 3(a,b). It shows quite different governing mechanism for traveling acoustic wave within the fluid comparing to results for copper pipe. The influence of wall elasticity significantly alters (decrease) the speed of sound (which is at zero frequency limit 470 ($+34/-25$ m/s at 95% confidence interval), as obtained from the map), while the structural damping causes wave attenuation. The dispersive waves appears in map as curved ridges that are asymptotic to the resonant frequency. In this map, the interaction between fluid mode and pipe mode waves is evident, characterizing the traveling wave acoustic phenomena. The correlation peaks vary, showing changes in scale. The time–frequency distribution of the magnitude of the WT peaks depends on frequency of group velocity. The wavelets at a position in time determine only the features of the signal near that position. Thus the changes in wavelets that correlate highly with the signal at different times indicate the changes in features of the signal at time progresses.

Similar values were obtained for another viscoelastic pipe material (PP—Fig. 4(a,b)), where the influence of wall elasticity also significantly decrease the speed of sound (which is at zero frequency limit 380 ($+32/-28$) m/s at 95% confidence interval). Since the speed of sound in fluid-filled pipe depends on pipe wall material, this changes the effective bulk modulus, as indicated in Eq. (15).

5. Conclusions

Time–frequency analysis such as wavelet transform (WT) can offer several advantages for velocity dispersion measurements in comparison to more traditional techniques. They can be applied to broadband signals so that one measurement may be required to determine the velocity of multiple modes over a wide range of frequencies. Another

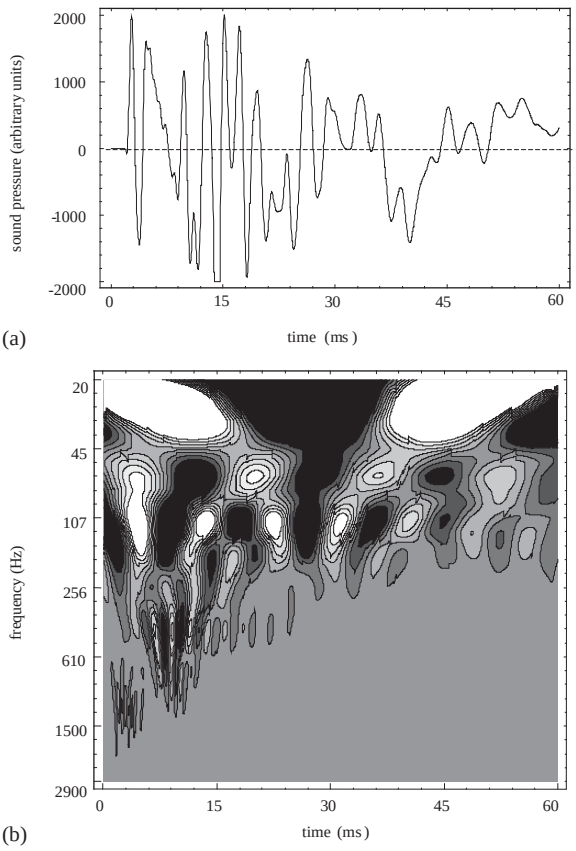

Fig. 4. Measured sound pressure signal and wavelet transform of signal in polypropylene (PP) pipe: (a) pressure signal; (b) wavelet transform.

important advantage is the ability to analyze signals containing multiple propagation modes and/or reflections which superimpose and interfere in the time domain. These multiple modes and reflections can be separated in time–frequency space. The WT also provides a direct measurement of group velocity dispersion.

The wavelet analysis was applied to the acoustic signal in order to analyze the structural features of the fluid-filled viscoelastic pipes. The WT characterize a one-dimensional acoustic signal as a two-dimensional representation, evolving with time and period (frequency). As a practical application to fluid-filled pipe, three different pipe wall materials were analyzed. The main object was to reveal the influence of physical properties of pipe wall material on acoustic wave propagation. From the analysis, the following conclusions are obtained.

Wavelet transform of acoustic signal enables the determination of the period (frequency) of signal at any time. In the wavelet coefficient map, signals of very different frequencies are displayed. Wavelet transform of non-stationary acoustic signal was used to measure the frequency-dependent fluid sound speed. A time–frequency map, constructed by plotting the wavelet coefficients against the time (translation) and scale parameter (period or frequency), shows an alteration of acoustic waves. The dominant features of each map are extracted by identifying correlation peaks. Each peak in WT map represents the arrival time of a wave traveling with the group velocity. Using the time–frequency distribution of the WT, the dependency on frequency of group velocity and attenuation is evaluated.

From the map is evident the influence of pipe material on acoustic waves. The influence of wall elasticity significantly alters (decrease) the speed of sound, while the structural damping causes wave attenuation. The dispersive waves appears in map as curved ridges that are asymptotic to the resonant frequency. Successive reflections appear in the map as families of high wavelet coefficients at constant period (or frequency). By measuring the time separation between ridges at given frequency, the wave velocity at that frequency can be calculated. In the pipe with semi-rigid wall, the lowest order mode is truly a plane wave mode, but in the pipes with elastic walls, the lowest order mode exhibits a dispersive sound speed, which is at all frequencies significantly slower than the free field value.

The results also showed that, in the case of propagating small disturbances (such as acoustic disturbances), the pipe wall inertance has a minor influence on the wave propagation characteristics. The elastic reaction of the wall to expansion of the cross-section greatly exceeds the inertial reactions.

References

Andria, G., Savino, M., Trotta, A., 1994. Application of Wigner-Ville distribution to measurement on transient signals. IEEE Transactions on Instrumentation and Measurements 43, 187–193.

Fanelli, M., 1973. Hydraulic Resonance in Rock-Bored Penstocks. Water Power 25, 342–346.

Fanelli, M., Angelico, G., Escobar, P., 1983. Comprehensive Experimental Confirmation of Transfer Matrix Theory for Uniform Pipelines under Steady Pulsating Conditions. In: Proceedings of 4th International Conference on Pressure Surges, Bath, pp. 214–219.

Farge, M., 1992. Wavelet transforms and their application to turbulence. Annual Review of Fluid Mechanics 24, 397–457.

Farge, M., Kavlahan, N., Perrier, V., Goirand, E., 1996. Wavelets and turbulence. Proceedings of the IEEE 4, 639–669.

Franke, P.-G., Seyler, F., 1983. Computation of unsteady pipe flow with respect to visco-elastic material properties. Journal of Hydraulic Research 21, 345–353.

Galley, M., Güney, M.S., Rieutord, E., 1979. An investigation of pressure transients in viscoelastic pipes. Journal of Fluids Engineering 101, 495–499.

Ghilardi, P., Paoletti, A., 1986. Additional viscoelastic pipes as pressure surges suppressors. In: Proceedings of 5th International Conference on Pressure Surges, Hannover, pp. 113–121.

Grossmann, A., Morlet, J., 1984. Decomposition of Hardy functions into square integrable wavelets of constant shape. Journal on Mathematical Analysis 4, 723–736.

Güney, M.S., 1983. Water hammer in viscoelastic pipes where cross-section parameters are time dependent. In: Proceedings of 4th International Conference on Pressure Surges, Bath, pp. 189–204.

Hirschmann, P., 1979. Resonanz in visko-elastischen Druckleitungen. Mitteilung der Institut für Hydraulik und Gewässerkunde, Technische Universität München, München, Germany.

Mallat, S., 1999. A Wavelet Tour of Signal Processing 2nd Edition. Academic Press, New York.

Martin, W., Flandrin, P., 1985. Wigner-Ville spectral analysis of nonstationary processes. IEEE Transactions on Acoustics, Speech and Signal Processing 33, 1461–1470.

Meissner, E., 1976. Berechnung Instationärer Strmungsforgänge in Kunststoffleitungen. Mitteilung der Institut für Hydraulik und Gewässerkunde, Technische Universität München, München, Germany.

Morlet, J., Arens, G., Furgeau, I., Giard, D., 1982. Wave propagation and sampling theory. Geophysics 2, 203–236.

Munjal, M.L., Thawani, P.T., 1996. Acoustic performance of hoses—a parametric study. Noise Control Engineering Journal 44, 274–280.

Munjal, M.L., Thawani, P.T., 1997. Prediction of the vibro-acoustic transmission loss of planar hose-pipe systems. Journal of Acoustical Society of America 101, 2524–2535.

Newland, D.E., 1994. Wavelet analysis of vibration: Part 1. Journal of Vibration and Acoustics 116, 409–416.

Newland, D.E., 1999. Ridge and phase identification in frequency analysis of transient signals by harmonic wavelets. Journal of Vibration and Acoustics 121, 149–155.

Rieutord, E., Blanchard, A., 1979. Pulsating viscoelastic pipe flow—water hammer. Journal of Hydraulic Research 17, 217–229.

Suo, L., Wylie, E.B., 1989. Impulse response methods for frequency-dependent pipeline transients. Journal of Fluids Engineering 111, 478–483.

Suo, L., Wylie, E.B., 1990. Complex wave speed and hydraulic transients in viscoelastic pipes. Journal of Fluids Engineering 112, 496–500.

Yu, J., Kojima, E., 1998. Wave propagation in fluids contained in finite-length anisotropic viscoelastic pipes. Journal of Acoustical Society of America 104, 3227–3235.